


Two-Qubit Operations for Finite-Energy Gottesman-Kitaev-Preskill Encodings

Ivan Rojko^{Ⓧ,*}, Paul Moser Röggl, Martin Wagener, Moritz Fontboté-Schmidt,
Stephan Welte, Jonathan Home, and Florentin Reiter^{Ⓧ,†}

*Institute for Quantum Electronics, ETH Zürich, Otto-Stern-Weg 1, 8093 Zürich, Switzerland
and Quantum Center, ETH Zürich, 8093 Zürich, Switzerland*

 (Received 25 May 2023; revised 27 March 2024; accepted 15 July 2024; published 3 September 2024)

We present techniques for performing two-qubit gates on Gottesman-Kitaev-Preskill (GKP) codes with finite energy, and find that operations designed for ideal infinite-energy codes create undesired entanglement when applied to physically realistic states. We demonstrate that this can be mitigated using recently developed local error-correction protocols, and evaluate the resulting performance. We also propose energy-conserving finite-energy gate implementations which largely avoid the need for further correction.

DOI: [10.1103/PhysRevLett.133.100601](https://doi.org/10.1103/PhysRevLett.133.100601)

The realization of a fault-tolerant quantum computer requires the implementation of a universal set of gates performed on error-corrected encoded logical qubits [1]. Encoding involves the redundant use of a larger Hilbert space, which is often obtained by mapping information across multiple physical systems. An alternative is to examine systems with an extended Hilbert space such as harmonic oscillators, of which bosonic codes [2] are a prominent example. One candidate set of bosonic codes are the Gottesman-Kitaev-Preskill (GKP) codes [3], in which quantum error correction has recently been demonstrated in both superconducting circuits [4,5] and trapped ions [6–8] using a single oscillator. In order to embed this encoding into a larger system [9–13], gates between multiple encoded qubits will be required. While multiqubit gate schemes have been proposed [3,14–17], these consider the action on “ideal” infinite-energy GKP states, with the effect on experimentally realizable finite-energy states treated as a tolerable source of error. However, recent theoretical [18,19] and experimental [8] works have shown that single-qubit operations can be designed for finite-energy states, which asks the question whether similar strategies can be taken for multiqubit gates.

In this Letter, we present two approaches to tackle this problem. First, we examine the effect of ideal, i.e., infinite-energy, two-qubit operations on finite-energy GKP states, and show that although the gate operation leads to significant distortion of the states, this is of a form which is correctable by finite-energy error-correction protocols. Second, we introduce direct finite-energy gates which preserve the energy of the states, and thus avoid the need for correction steps. These components serve as a

foundation for integrating finite-energy GKP states into larger-scale quantum computing systems, providing a path towards fault-tolerant processing of quantum information.

GKP encodings have a characteristic gridlike structure in phase space and are defined through displacement operators. The logical Pauli operators and the stabilizers for a square code are defined by $\hat{X} = e^{i\hat{p}\sqrt{\pi}}$, $\hat{Z} = e^{-i\hat{q}\sqrt{\pi}}$ and $\hat{S}_x = e^{i\hat{p}^2\sqrt{\pi}}$, $\hat{S}_z = e^{-i\hat{q}^2\sqrt{\pi}}$, respectively [20]. The simultaneous eigenstates of these operators are the ideal GKP codewords $|\mu\rangle_{\text{I}} = \sum_s |q = (2s + \mu)\sqrt{\pi}\rangle$, where $\mu \in \{0, 1\}$, $s \in \mathbb{Z}$ and the subscript “I” stands for *ideal*. Since each component of the superposition is an infinitely squeezed state, ideal codewords have an infinite norm and are thus not physical. A finite-energy version of these states can be constructed using a Gaussian phase-space envelope centered at the origin [3,14,18,21,22]. Mathematically, this can be realized by introducing an envelope operator $\hat{E}_{\Delta} = e^{-\Delta^2 \hat{n}}$, where $\hat{n} = \frac{1}{2}(\hat{q}^2 + \hat{p}^2)$ is the number operator and Δ parametrizes the size of the code states in phase space. A finite-energy GKP state is then expressed by $|\psi\rangle_{\Delta} \propto \hat{E}_{\Delta} |\psi\rangle_{\text{I}}$ and can be thought of as a superposition of periodically spaced, finitely squeezed states weighted according to an overall Gaussian envelope. The states and their marginal distributions, $P(x) = |\langle x|0\rangle_{\Delta}|^2$ with $x \in \{q, p\}$, are thus characterized by two parameters; the peak’s standard deviation Δ_{peak} and the inverse of the Gaussian envelope’s standard deviation Δ_{envl} . For a pure state $|\psi\rangle_{\Delta}$, these are both equal to Δ .

Two-qubit entangling gates are essential operations for universal quantum computation [23]. For GKP codes, such gates can be realized using quadrature–quadrature coupling Hamiltonians that are equivalent to each other up to local phase-space transformations. Here we focus on the controlled \hat{Z} gate, a two-qubit operation expressed as $CZ = e^{i\hat{q}_1 \hat{q}_2}$ [3,14], where the indices 1 and 2 denote the

*Contact author: irojko@phys.ethz.ch

†Contact author: freiter@phys.ethz.ch

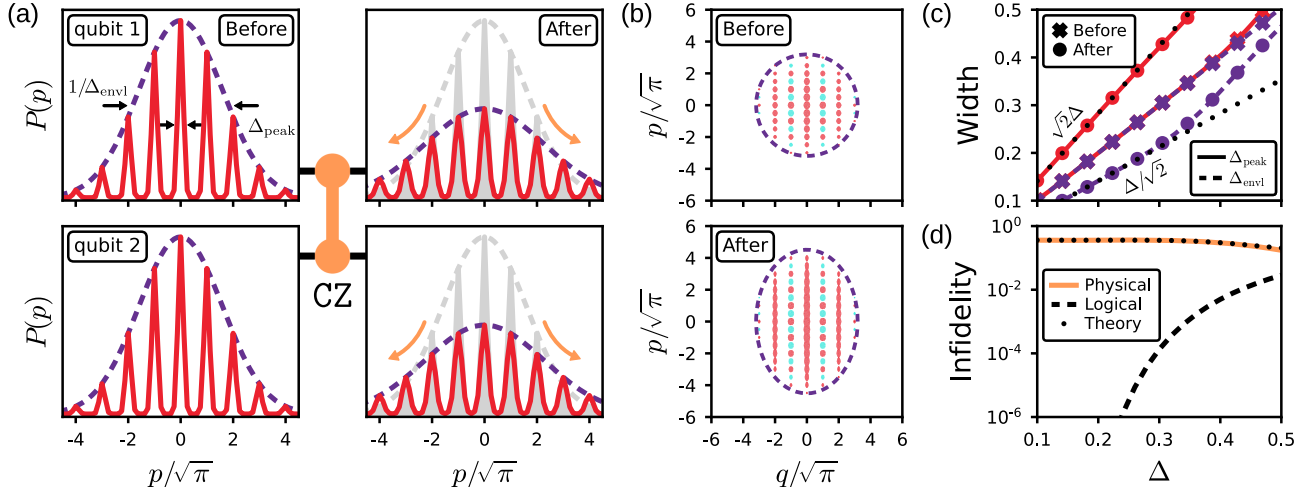


FIG. 1. Finite-energy effects in two GKP qubit operations. (a) Momentum marginal distribution $P(p)$ of both oscillators starting in the state $|0\rangle_{\Delta}$ before (left) and after (right) the CZ gate. The output distributions get broadened as the operation corresponds to a continuous set of displacements that spreads each oscillator’s wave function conditioned on the position of the other one. (b) Wigner quasiprobability distribution, showing broadening only in the p quadrature. (c) Peak widths as a function of input width, showing clearly the linear relation. (d) The physical and logical infidelity between the input and output states as a function of the energy parameter Δ .

two oscillators. The action of CZ on position eigenstates, $|q_1 = m_1\sqrt{\pi}\rangle|q_2 = m_2\sqrt{\pi}\rangle$, is to add in a prefactor $e^{-izm_1m_2}$ with m_1, m_2 being either odd or even integers. If the input state is $|1\rangle_1|1\rangle_1$ the system acquires an overall phase of π , whereas all other input states acquire a multiple of 2π .

Because of their limited extent in phase space, finite-energy GKP states are not translationally invariant and thus the action of the CZ gate described above produces distortion of the underlying states. Consider the situation depicted in Fig. 1(a); from the perspective of the second subsystem the gate corresponds to a series of displacements $\sum_{q_1} \langle q_1 | \text{CZ} | q_1 \rangle = \sum_{q_1} e^{iq_1\hat{q}_2} \equiv \sum_{q_1} \hat{D}_2(iq_1/\sqrt{2})$. Each of these displacements shifts both the individual Gaussian peaks and the envelope of the state. The final subsystem state can thus be regarded as a Gaussian mixture model, i.e., a weighted sum of Gaussian functions with a broader envelope and peak width. This distortion occurs only in the p quadrature [see Fig. 1(b)].

In order to analytically quantify the broadening of the envelope we evaluate the marginal distribution of the first oscillator after tracing out the second one from the state following the gate: $P(p_1) = \langle p_1 | \text{Tr}_2[\text{CZ}\rho_{\Delta}\text{CZ}^{\dagger}] | p_1 \rangle$, where $\rho_{\Delta} = |00\rangle_{\Delta\Delta}\langle 00|$. We perform this calculation using the shifted grid state representation [3,24–28] and recognizing that the main additional contributions come from the first nearest neighbor peaks (see Supplemental Material [29]). This assumption is valid for GKP states with $\Delta \lesssim 0.4$ which is consistent with recent experimental realizations [4,5,8]. The marginal distribution of the target state after the gate retains a finite-energy GKP form but with characteristic parameters being updated to

$$\Delta_{\text{peak}}^2 = 2\Delta^2 \quad \text{and} \quad \Delta_{\text{envl}}^2 = \frac{\Delta^2}{2}. \quad (1)$$

Thus both the peak and envelope widths of the marginal distribution after the CZ gate increase by a factor of $\sqrt{2}$ compared to their initial values. Figure 1(c) shows the comparison between these input and output state parameters. Eq. (1) is accurate to $\mathcal{O}(\Delta^6)$, but further improvements can be made by including contributions from subsequent neighboring peaks using the same method. Analytical expressions for the position marginal distributions and the purity of each subsystem are discussed further in the Supplemental Material [29].

An alternative measure of the quality of a given GKP code are the effective squeezing parameters [26,27,54], which are defined as $\sigma_{x/z}^2 = (1/\pi) \log(|\text{Tr}[\hat{S}_{x/z}\rho]|^{-2})$ and quantify the closeness of a system’s state ρ to the unit eigenstates of the code stabilizers. In ideal GKP states, both effective squeezing parameters are 0, while for pure finite-energy states such as $|0\rangle_{\Delta}$, $\sigma_{x/z} = \Delta$. After the CZ gate is applied, we find that the effective squeezing parameters of each subsystem read $\sigma_x = \sqrt{2}\Delta$ and $\sigma_z = \Delta$. The former expression is consistent with the peak and envelope broadening in $P(p_1)$ of Eq. (1). The expression for σ_z indicates that the marginal distribution in the position space will be unaffected by the gate.

The main consequence of these finite-energy modifications is the lowering of the physical overlap fidelity between the input and desired output states, $F = |\langle \psi_{\text{out}} | \text{CZ} | \psi_{\text{in}} \rangle|^2$. As an example, we derive this quantity for the input state $|00\rangle_{\Delta}$ using as above the shifted

grid state method and the first nearest neighbor assumption, obtaining

$$F \approx \frac{16}{25} \frac{\left(1 + 4e^{-\frac{\pi}{5\Delta^2}}\right)^2}{\left(1 + 2e^{-\frac{\pi}{\Delta^2}}\right)^4 \left(1 + 2e^{-\frac{\pi}{4\Delta^2}}\right)^4}. \quad (2)$$

Figure 1(d) shows that this expression agrees with the numerically evaluated overlap using state vector simulations. Eq. (2) provides an accurate approximation of the true fidelity up to $\mathcal{O}(\Delta^3)$ (a higher-order formula and the fidelity for other states can be found in Supplemental Material [29]). In the limit $\Delta \rightarrow 0$ the fidelity approaches a finite value $F_{\max} = 16/25 = 0.64$, which is independent of the input state. Despite converging to ideal codewords, GKP states with $\Delta^2 \ll 1$ still possess finite-width peaks and envelope which remain susceptible to broadening due to the two-qubit interaction. The logical fidelity which for the state $|00\rangle_\Delta$ is accessible by integrating its position marginal distribution over $[-\sqrt{\pi}/2; \sqrt{\pi}/2] + 2\sqrt{\pi}\mathbb{Z}$ remains close to unity [16,24,55].

The CZ gate operation considered above can be realized exactly using two beam splitters and a single layer of single-mode squeezers [15,16]. We find that it is also possible to achieve the same interaction using an alternative decomposition consisting of two squeezing operations and only one application of the beam splitter. This is given by $\text{CZ}(\theta, r) = \hat{S}^{\otimes 2}(r) \hat{B}_A(\theta) \hat{S}^{\otimes 2}(-r)$ with $\hat{S}^{\otimes 2}(r) = \hat{S}(r) \otimes \hat{S}(r)$ and $\hat{S}(r) = e^{i\frac{1}{2}r(\hat{q}_j \hat{p}_j + \hat{p}_j \hat{q}_j)}$, representing the squeezing operation on mode j , while $\hat{B}_A(\theta) = e^{i\theta(\hat{q}_1 \hat{q}_2 + \hat{p}_1 \hat{p}_2)}$ is the antisymmetric beam splitter transformation. This chain of operations can then be written as

$$\text{CZ}(\theta, r) = e^{i\theta(e^{2r}\hat{q}_1\hat{q}_2 + e^{-2r}\hat{p}_1\hat{p}_2)}. \quad (3)$$

The ideal desired gate is obtained when $\theta = e^{-2r}$ and $r \rightarrow \infty$, which makes this decomposition a convergent but approximate realization of CZ. The Hilbert-Schmidt distance between the symplectic representations of $\text{CZ}(\theta, r)$ and CZ scales as $\sqrt{3}e^{-4r}$, which constitutes a deviation with respect to the ideal operator norm that is below 1% at $r > 1.06$. In practice, we find that the overlap fidelity F is above 0.6 for $r \geq 0.75$ and at $r = 1.0$ has less than 0.7% error relative to F_{\max} . The approximate decomposition in Eq. (3) has the advantage of requiring a weaker bilinear interaction than previously proposed schemes [15,16], allowing for a flexible selection of the beam splitter coupling strength complying with a fault-tolerant concatenation of GKP and surface codes, aiding in reducing the accumulation of errors during the gate time [12,29]. The limitation of this scheme is that it maintains squeezed quadratures for an extended duration, thereby enhancing the susceptibility of the GKP code to minor deviations. This decomposition as well as the previously proposed ones induce the same finite-energy effects as the ideal operation.

A first solution against finite-energy effects is to correct them locally, given that despite the impact of these effects on the state of the oscillators, the CZ gate effectively executes the intended logical operation. Using recently demonstrated quantum error correction (QEC) protocols [5,8,18], we show that this works. Figure 2(a) shows the protocol for the error-corrected CZ gate. We initialize the system in a pure state $\rho_{\text{in}} = |\psi_{\text{in}}\rangle_{\Delta\Delta} \langle\psi_{\text{in}}|$ and perform a series of finite-energy stabilization cycles that correct for small displacements in position and momentum and for deformations in the state's energy envelope. Halfway through the series of QEC rounds we perform the CZ gate and resume the stabilization. After each correction round before the gate, we evaluate the overlap fidelity as $F(\rho, |\psi_{\text{in}}\rangle_\Delta)$, whereas for those after the CZ we use $F(\rho, |\psi_{\text{out}}\rangle_\Delta)$ with $F(\rho, |\psi\rangle) = \langle\psi|\rho|\psi\rangle$ and $|\psi_{\text{out}}\rangle_\Delta \propto \hat{E}_\Delta \text{CZ} |\psi_{\text{in}}\rangle_I$ being the desired output state. As an example, Fig. 2(b) illustrates this quantity for $|\psi_{\text{in}}\rangle_\Delta = |00\rangle_\Delta = |\psi_{\text{out}}\rangle_\Delta$ as a function of the correction round. As anticipated, the gate lowers the fidelity, but after a few rounds of error correction the fidelity recovers.

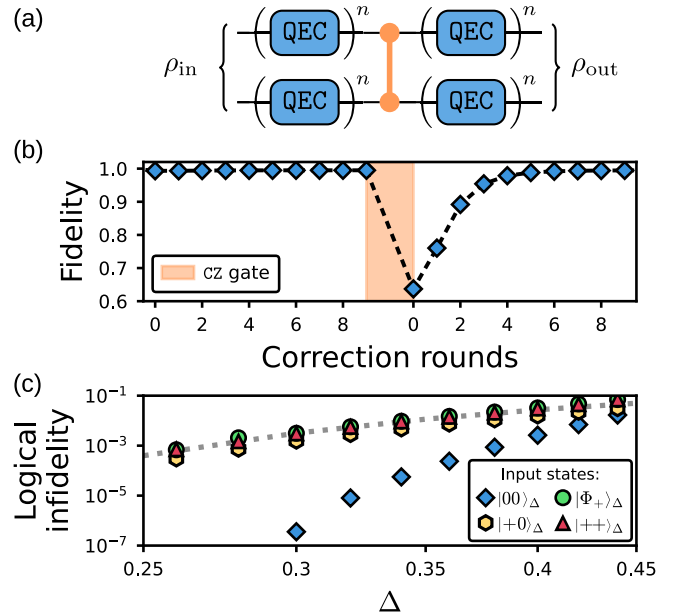


FIG. 2. Correction of finite-energy effects. (a) The circuit representation of the error-corrected CZ gate. The system is initialized in a state $\rho_{\text{in}} = |\psi_{\text{in}}\rangle_{\Delta\Delta} \langle\psi_{\text{in}}|$ and undergoes n stabilization cycles. After $n = 9$ rounds, the ideal CZ gate is applied, followed by $n = 9$ additional rounds of correction. (b) Fidelity F evaluated after each QEC round with $|\psi_{\text{in}}\rangle_\Delta = |00\rangle_\Delta$ and $\Delta = 0.3$. (c) The logical infidelity as a function of Δ evaluated as the difference of overlap fidelities at the 9th round of QEC before and after CZ. Before the gate, the overlap fidelity is obtained with $F(\rho, |\psi_{\text{in}}\rangle_\Delta)$, whereas after CZ using $F(\rho, |\psi_{\text{out}}\rangle_\Delta)$, where $|\psi_{\text{out}}\rangle_\Delta$ is the desired output state which for each input state corresponds to $|00\rangle_\Delta$, $|+0\rangle_\Delta$, $|\Phi_-\rangle_\Delta$ or $(|0+\rangle_\Delta + |1-\rangle_\Delta)/\sqrt{2}$, respectively. The dotted curve represents the analytical result from Eq. (4).

To quantify the logical infidelity we evaluate $F(\rho_b, |\psi_{in}\rangle_\Delta) - F(\rho_{out}, |\psi_{out}\rangle_\Delta)$ with ρ_b and ρ_{out} being the states before the gate and after the entire protocol. We observe that this difference is finite [see Fig. 2(c)]. This is explained by the distortion in phase space of both oscillators' state that then increases the probability that the finite-energy stabilization procedure misinterprets $|0\rangle_\Delta$ for $|1\rangle_\Delta$ (and vice versa). The states with logical coherences, e.g., $|+\rangle_\Delta$, are the most affected by this distortion because their information is primarily stored in the momentum quadrature. Therefore, we observe that the logical infidelity for states such as $|+0\rangle_\Delta$, $|++\rangle_\Delta$, or the Bell state $|\Phi_+\rangle_\Delta \propto |00\rangle_\Delta + |11\rangle_\Delta$ is several orders of magnitude higher than for the computational states. We can approach the infidelity for those states using some ideal decoders [29] or by integrating appropriate marginal distributions. Taking $|+0\rangle_\Delta$ as the analytically simplest example, we construct $P(p_1)$ using peaks and envelope widths derived in Eq. (1) and integrate it over the domain $[-\sqrt{\pi}/2; \sqrt{\pi}/2] + 2\sqrt{\pi}Z$ to obtain

$$1 - F_{\text{logic}} \approx \frac{2\sqrt{2}\Delta}{\pi} e^{-\frac{\pi}{8\Delta^2}} \left(1 - \frac{4\Delta^2}{\pi}\right), \quad (4)$$

which is accurate to $\mathcal{O}(\Delta^5)$. This expression is illustrated by the dashed curve in Fig. 2(c). Despite this undesired behavior, the infidelity of the stabilized CZ gate for states with $\Delta \leq 0.34$ is below 1%, a value that has been shown to be sufficient for a fault-tolerant concatenation of GKP codes with discrete variable encodings [13]. The performance of the error-corrected gate can be enhanced by improving the recovery procedure using reshaping of GKP states into a rectangular lattice [18] or postselection based on correlation in syndrome outcomes between multiple rounds of QEC [5] (see Supplemental Material [29]).

An alternative to local error correction is to use a finite-energy version of the gate which minimally distorts physical GKP states [8,14,18]. The finite-energy form of the CZ gate is the nonunitary interaction $\text{CZ}_\Delta = \hat{E}_\Delta \text{CZ} \hat{E}_\Delta^{-1} = e^{i\hat{q}_1 \hat{q}_2 - \Delta^2 (\hat{q}_1 \hat{p}_2 + \hat{p}_1 \hat{q}_2)}$ whose implementation requires us to couple the two oscillators to some auxiliary system. Inspired by a collisional model of dissipation [56] and a block encoding of the nonunitary operation [57], we approximate CZ_Δ by a unitary operation $e^{i\hat{q}_1 \hat{q}_2 \hat{\sigma}_x - i\Delta^2 (\hat{q}_1 \hat{p}_2 + \hat{p}_1 \hat{q}_2) \hat{\sigma}_y}$ followed by a reset of the auxiliary spin. The Trotterized version of this operation is realizable through spin-conditioned beam splitters and/or squeezing [29]. Unfortunately, this engineered dissipative dynamics is subject to approximation errors. As a consequence, the fidelity that one reaches with the 1st order Trotter formula is 0.80 when $\Delta^2 \ll 1$, an improvement of only 0.16 compared to the ideal CZ gate. Higher order formulas entail a significant increase in the number of operations and complexity of the gate.

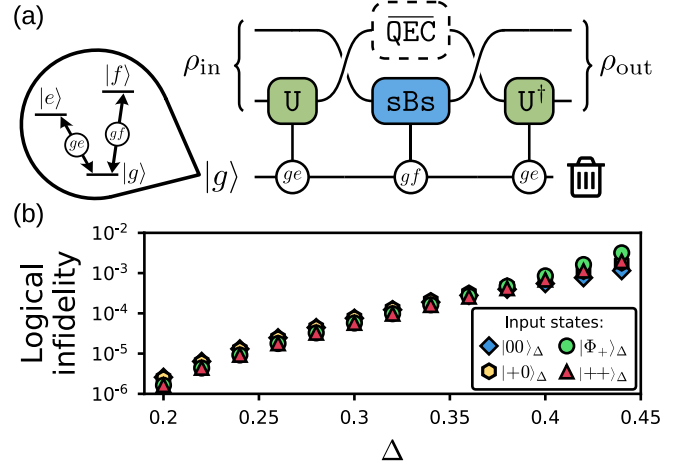


FIG. 3. Two-qubit gate mediated by an auxiliary three-level system. (a) Circuit representation of the protocol. The system is initialized in a state ρ_{in} . The auxiliary system starting in $|g\rangle$ is used to retrieve the logical information of one of the oscillators using CU after what the two oscillators are swapped using a 50:50 beam splitter. sBs represents a finite-energy stabilization which also effects a Pauli Z operation if the qutrit is in $|g\rangle$. The circuit is then reversed in order to disentangle the oscillators from the auxiliary system. (b) The logical infidelity evaluated in a similar fashion as in Fig. 2(c).

To achieve higher fidelities, we propose a third approach that involves employing an auxiliary three-level system coupled to only one of the oscillators. In this hybrid discrete-continuous variable system we use the qutrit to facilitate quantum information exchange between the two oscillators. To entangle two GKP states, we first query the logical information of the initial oscillator using the auxiliary system, then swap bosonic states and apply an operation on the second oscillator conditioned on the auxiliary state. Finally, we swap the bosonic states back and disentangle the first oscillator from the auxiliary system. This procedure is illustrated in Fig. 3(a). Since the swap via two 50:50 beam splitters is intrinsically finite energy, the scheme preserves the states' energy as long as the conditional CU and sBs are finite energy. The former operation reads $\text{CU} = e^{-il\hat{q}\hat{\sigma}_y^{(ge)}} e^{-il\Delta^2 \hat{p}\hat{\sigma}_x^{(ge)}}$ with $l = \sqrt{\pi}/2$ and is identical to the unitary used for the readout of finite-energy GKP states proposed in Refs. [8,19]. With $\hat{\sigma}_x^{(ge)}$ and $\hat{\sigma}_y^{(ge)}$ being Pauli operators between states $|g\rangle$ and $|e\rangle$ of the qutrit, this operation entangles those states with $|0\rangle_\Delta$ and $|1\rangle_\Delta$, respectively. The second operation is the so-called small-Big-small circuit $\text{sBs} = e^{-il\Delta^2 \hat{p}\hat{\sigma}_y^{(af)}} e^{il\hat{q}\hat{\sigma}_x^{(af)}} e^{-il\Delta^2 \hat{p}\hat{\sigma}_y^{(af)}}$ which has been used to perform measurement-free error correction of the position quadrature of GKP states [8,18]. On top of the corrective power sBs has the property to apply a logical Pauli Z that we use to add a phase to the oscillator state if the auxiliary system is in $|g\rangle$. The final operation is the inverse of the first one followed by a reset

of the qutrit. The logical infidelity of this scheme shown in Fig. 3(b) is consistent across states and lower than that of the error-corrected gate. For comparison for $\Delta \leq 0.34$ the fidelity is below 0.01%. The main source of this infidelity stems from CU and CU^\dagger , which can be mitigated by correcting the first oscillator state in between the two swaps. After CU, the GKP state is no longer stabilized by (\hat{S}_x, \hat{S}_z) but by $(-\hat{S}_x, \hat{S}_z)$. Fortunately, autonomous error correction protocol can be adapted to this new stabilizer set [represented as $\overline{\text{QEC}}$ in Fig. 3(a)] [29].

All the required elements, such as beam splitters and squeezers, for realizing both ideal and finite-energy two GKP qubit operations have been successfully demonstrated in experimental setups utilizing trapped ions [58–66] and superconducting microwave cavities [67–74]. In Supplemental Material [29], we provide details on experimental requirements for a trapped ion system.

Our work addresses a critical issue in continuous-variable quantum information processing by proposing protocols to address the fidelity loss issue in two-qubit gates between GKP qubits. To this end we use quantum error correction, introduce a direct construction of finite-energy two-qubit gate, and propose a protocol relying on an auxiliary three-level system to mediate the logical information between oscillators. Our proposed solutions can be made fault tolerant: This could be addressed through the use of biased-noise auxiliary systems [30] or multiple discrete-variable systems, offering the potential for fault tolerance through the utilization of flag qubits, detection or correction codes, or path-independent gate technique [75–77]. While this has been suggested using bosonic biased systems such as Cat codes, further work is necessary to investigate how to incorporate these methods into multiqubit GKP gates offering a path towards fault tolerance using hybrid discrete-continuous variable codes [78]. Another important question for later study is how the finite-energy effects of ideal two-qubit gates together with standard continuous-variable noise processes, such as photon loss and dephasing, modify the thresholds of GKP-based encodings [10–13]. We believe that our findings will contribute to the use of GKP codes for fault-tolerant quantum computation using dissipative QEC [8,79] as well as for applications such as error-corrected quantum sensing [54] that is bias free [80].

Acknowledgments—I. R. thanks Daniel Weigand for the extensive and helpful discussion on the shifted grid state method, Brennan de Neeve for numerous discussions on GKP codes, and Elias Zapusek for insightful questions throughout the project. This work was supported as a part of NCCR QSIT, a National Centre of Competence (or Excellence) in Research, funded by the Swiss National Science Foundation (SNSF) Grant No. 51NF40-185902. I. R. and F. R. acknowledge financial support via the SNSF Ambizione Grant No. PZ00P2_186040. M. W.

acknowledges support via the SNSF research Grant No. 200020_179147. S. W. acknowledges financial support via the SNSF Swiss Postdoctoral Fellowship Grant No. TMPFP2_210584.

-
- [1] D. Gottesman, [arXiv:0904.2557](https://arxiv.org/abs/0904.2557).
 - [2] V. V. Albert and P. Faist, in *The Error Correction Zoo*, <https://errorcorrectionzoo.org/c/oscillators> (2022).
 - [3] D. Gottesman, A. Kitaev, and J. Preskill, *Phys. Rev. A* **64**, 012310 (2001).
 - [4] P. Campagne-Ibarcq, A. Eickbusch, S. Touzard, E. Zalys-Geller, N. E. Frattini, V. V. Sivak, P. Reinhold, S. Puri, S. Shankar, R. J. Schoelkopf, L. Frunzio, M. Mirrahimi, and M. H. Devoret, *Nature (London)* **584**, 368 (2020).
 - [5] V. V. Sivak, A. Eickbusch, B. Royer, S. Singh, I. Tsioutsios, S. Ganjam, A. Miano, B. L. Brock, A. Z. Ding, L. Frunzio, S. M. Girvin, R. J. Schoelkopf, and M. H. Devoret, *Nature (London)* **616**, 50 (2023).
 - [6] C. Flühmann, T. L. Nguyen, M. Marinelli, V. Negnevitsky, K. Mehta, and J. P. Home, *Nature (London)* **566**, 513 (2019).
 - [7] C. Flühmann and J. P. Home, *Phys. Rev. Lett.* **125**, 043602 (2020).
 - [8] B. de Neeve, T.-L. Nguyen, T. Behrle, and J. P. Home, *Nat. Phys.* **18**, 296 (2022).
 - [9] N. C. Menicucci, P. van Loock, M. Gu, C. Weedbrook, T. C. Ralph, and M. A. Nielsen, *Phys. Rev. Lett.* **97**, 110501 (2006).
 - [10] K. Fukui, A. Tomita, A. Okamoto, and K. Fujii, *Phys. Rev. X* **8**, 021054 (2018).
 - [11] C. Vuillot, H. Asasi, Y. Wang, L. P. Pryadko, and B. M. Terhal, *Phys. Rev. A* **99**, 032344 (2019).
 - [12] K. Noh and C. Chamberland, *Phys. Rev. A* **101**, 012316 (2020).
 - [13] K. Noh, C. Chamberland, and F. G. S. L. Brandão, *PRX Quantum* **3**, 010315 (2022).
 - [14] N. C. Menicucci, *Phys. Rev. Lett.* **112**, 120504 (2014).
 - [15] B. M. Terhal, J. Conrad, and C. Vuillot, *Quantum Sci. Technol.* **5**, 043001 (2020).
 - [16] I. Tzitrin, J. E. Bourassa, N. C. Menicucci, and K. K. Sabapathy, *Phys. Rev. A* **101**, 032315 (2020).
 - [17] B. W. Walshe, B. Q. Baragiola, R. N. Alexander, and N. C. Menicucci, *Phys. Rev. A* **102**, 062411 (2020).
 - [18] B. Royer, S. Singh, and S. M. Girvin, *Phys. Rev. Lett.* **125**, 260509 (2020).
 - [19] J. Hastrup and U. L. Andersen, *Quantum Sci. Technol.* **6**, 035016 (2021).
 - [20] For other code geometries, the analysis and results will be similar after linearly transforming the quadratures.
 - [21] K. R. Motes, B. Q. Baragiola, A. Gilchrist, and N. C. Menicucci, *Phys. Rev. A* **95**, 053819 (2017).
 - [22] K. Noh, V. V. Albert, and L. Jiang, *IEEE Trans. Inf. Theory* **65**, 2563 (2019).
 - [23] M. J. Bremner, C. M. Dawson, J. L. Dodd, A. Gilchrist, A. W. Harrow, D. Mortimer, M. A. Nielsen, and T. J. Osborne, *Phys. Rev. Lett.* **89**, 247902 (2002).
 - [24] S. Glancy and E. Knill, *Phys. Rev. A* **73**, 012325 (2006).

- [25] A. Ketterer, A. Keller, S. P. Walborn, T. Coudreau, and P. Milman, *Phys. Rev. A* **94**, 022325 (2016).
- [26] B. M. Terhal and D. Weigand, *Phys. Rev. A* **93**, 012315 (2016).
- [27] D. J. Weigand and B. M. Terhal, *Phys. Rev. A* **97**, 022341 (2018).
- [28] T. Matsuura, H. Yamasaki, and M. Koashi, *Phys. Rev. A* **102**, 032408 (2020).
- [29] See Supplemental Material at <http://link.aps.org/supplemental/10.1103/PhysRevLett.133.100601>, which includes Refs. [30–53], for more detailed derivations of the results presented in the main text and their extension to states with a non-symmetric energy envelope in q and p .
- [30] A. L. Grimsmo and S. Puri, *PRX Quantum* **2**, 020101 (2021).
- [31] K. V. Mardia and P. E. Jupp, *Directional Statistics*, Wiley Series in Probability and Statistics (John Wiley, Chichester, New York, 2000).
- [32] V. V. Albert, K. Noh, K. Duivenvoorden, D. J. Young, R. T. Brierley, P. Reinhold, C. Vuillot, L. Li, C. Shen, S. M. Girvin, B. M. Terhal, and L. Jiang, *Phys. Rev. A* **97**, 032346 (2018).
- [33] B. Q. Baragiola, G. Pantaleoni, R. N. Alexander, A. Karanjai, and N. C. Menicucci, *Phys. Rev. Lett.* **123**, 200502 (2019).
- [34] J. Hastrup, K. Park, J. B. Brask, R. Filip, and U. L. Andersen, *npj Quantum Inf.* **7**, 1 (2021).
- [35] C. Weedbrook, S. Pirandola, R. García-Patrón, N. J. Cerf, T. C. Ralph, J. H. Shapiro, and S. Lloyd, *Rev. Mod. Phys.* **84**, 621 (2012).
- [36] S. L. Braunstein, *Phys. Rev. A* **71**, 055801 (2005).
- [37] J. Zak, *Phys. Rev. Lett.* **19**, 1385 (1967).
- [38] L. J. Mensen, B. Q. Baragiola, and N. C. Menicucci, *Phys. Rev. A* **104**, 022408 (2021).
- [39] S. Lloyd and S. L. Braunstein, *Phys. Rev. Lett.* **82**, 1784 (1999).
- [40] C. Bloch and A. Messiah, *Nucl. Phys.* **39**, 95 (1962).
- [41] G. Cariolaro and G. Pierobon, *Phys. Rev. A* **94**, 062109 (2016).
- [42] V. V. Sivak, N. E. Frattini, V. R. Joshi, A. Lingenfelter, S. Shankar, and M. H. Devoret, *Phys. Rev. Appl.* **11**, 054060 (2019).
- [43] P. C. Haljan, K.-A. Brickman, L. Deslauriers, P. J. Lee, and C. Monroe, *Phys. Rev. Lett.* **94**, 153602 (2005).
- [44] C. H. Bennett, D. P. DiVincenzo, J. A. Smolin, and W. K. Wootters, *Phys. Rev. A* **54**, 3824 (1996).
- [45] W. K. Wootters, *Phys. Rev. Lett.* **80**, 2245 (1998).
- [46] C. Gardiner and P. Zoller, *Quantum Noise: A Handbook of Markovian and Non-Markovian Quantum Stochastic Methods with Applications to Quantum Optics*, 3rd ed., Springer Series in Synergetics (Springer-Verlag, Berlin Heidelberg, 2004).
- [47] N. Hatano and M. Suzuki, in *Quantum Annealing and Other Optimization Methods*, Lecture Notes in Physics, edited by A. Das and B. K. Chakrabarti (Springer, Berlin, Heidelberg, 2005), pp. 37–68.
- [48] H. C. J. Gan, G. Maslennikov, K.-W. Tseng, C. Nguyen, and D. Matsukevich, *Phys. Rev. Lett.* **124**, 170502 (2020).
- [49] M. H. Shaw, A. C. Doherty, and A. L. Grimsmo, *PRX Quantum* **5**, 010331 (2024).
- [50] D. Layden, *Phys. Rev. Lett.* **128**, 210501 (2022).
- [51] I. Rojkov, CVsim.jl: Continuous Variable systems simulation (2024), [10.5281/zenodo.13127577](https://doi.org/10.5281/zenodo.13127577).
- [52] J. Bezanson, A. Edelman, S. Karpinski, and V. B. Shah, *SIAM Rev.* **59**, 65 (2017).
- [53] S. Krämer, D. Plankensteiner, L. Ostermann, and H. Ritsch, *Comput. Phys. Commun.* **227**, 109 (2018).
- [54] K. Duivenvoorden, B. M. Terhal, and D. Weigand, *Phys. Rev. A* **95**, 012305 (2017).
- [55] G. Pantaleoni, B. Q. Baragiola, and N. C. Menicucci, *Phys. Rev. Lett.* **125**, 040501 (2020).
- [56] F. Ciccarello, *Quantum Meas. Quantum Metro.* **4**, 53 (2017).
- [57] A. Gilyén, Y. Su, G. H. Low, and N. Wiebe, *Proceedings of the 51st Annual ACM SIGACT Symposium on Theory of Computing* (Association for Computing Machinery, New York, 2019), p. 193.
- [58] D. Leibfried, B. DeMarco, V. Meyer, M. Rowe, A. Ben-Kish, J. Britton, W. M. Itano, B. Jelenković, C. Langer, T. Rosenband, and D. J. Wineland, *Phys. Rev. Lett.* **89**, 247901 (2002).
- [59] K. R. Brown, C. Ospelkaus, Y. Colombe, A. C. Wilson, D. Leibfried, and D. J. Wineland, *Nature (London)* **471**, 196 (2011).
- [60] D. J. Gorman, P. Schindler, S. Selvarajan, N. Daniilidis, and H. Häffner, *Phys. Rev. A* **89**, 062332 (2014).
- [61] S. C. Burd, R. Srinivas, J. J. Bollinger, A. C. Wilson, D. J. Wineland, D. Leibfried, D. H. Slichter, and D. T. C. Allcock, *Science* **364**, 1163 (2019).
- [62] R. T. Sutherland and R. Srinivas, *Phys. Rev. A* **104**, 032609 (2021).
- [63] P.-Y. Hou, J. J. Wu, S. D. Erickson, D. C. Cole, G. Zarantonello, A. D. Brandt, A. C. Wilson, D. H. Slichter, and D. Leibfried, *Nat. Phys.* **1** (2024).
- [64] O. Katz, M. Cetina, and C. Monroe, *Phys. Rev. Lett.* **129**, 063603 (2022).
- [65] O. Katz, M. Cetina, and C. Monroe, *PRX Quantum* **4**, 030311 (2023).
- [66] Y. Shapira, S. Cohen, N. Akerman, A. Stern, and R. Ozeri, *Phys. Rev. Lett.* **130**, 030602 (2023).
- [67] A. Baust *et al.*, *Phys. Rev. B* **91**, 014515 (2015).
- [68] W. Pfaff, C. J. Axline, L. D. Burkhardt, U. Vool, P. Reinhold, L. Frunzio, L. Jiang, M. H. Devoret, and R. J. Schoelkopf, *Nat. Phys.* **13**, 882 (2017).
- [69] M. C. Collodo, A. Potočnik, S. Gasparinetti, J.-C. Besse, M. Pechal, M. Sameti, M. J. Hartmann, A. Wallraff, and C. Eichler, *Phys. Rev. Lett.* **122**, 183601 (2019).
- [70] N. E. Frattini, V. V. Sivak, A. Lingenfelter, S. Shankar, and M. H. Devoret, *Phys. Rev. Appl.* **10**, 054020 (2018).
- [71] Y. Y. Gao, B. J. Lester, Y. Zhang, C. Wang, S. Rosenblum, L. Frunzio, L. Jiang, S. M. Girvin, and R. J. Schoelkopf, *Phys. Rev. X* **8**, 021073 (2018).
- [72] T. Hillmann, F. Quijandría, G. Johansson, A. Ferraro, S. Gasparinetti, and G. Ferrini, *Phys. Rev. Lett.* **125**, 160501 (2020).
- [73] B. J. Chapman, S. J. de Graaf, S. H. Xue, Y. Zhang, J. Teoh, J. C. Curtis, T. Tsunoda, A. Eickbusch, A. P. Read,

- A. Koottandavida, S. O. Mundhada, L. Frunzio, M. H. Devoret, S. M. Girvin, and R. J. Schoelkopf, *PRX Quantum* **4**, 020355 (2023).
- [74] I. Pietikäinen, O. Černotík, S. Puri, R. Filip, and S. M. Girvin, *Quantum Sci. Technol.* **7**, 035025 (2022).
- [75] Y. Shi, C. Chamberland, and A. Cross, *New J. Phys.* **21**, 093007 (2019).
- [76] J. Hastrup, K. Park, J. B. Brask, R. Filip, and U. L. Andersen, *Phys. Rev. Lett.* **128**, 110503 (2022).
- [77] W.-L. Ma, M. Zhang, Y. Wong, K. Noh, S. Rosenblum, P. Reinhold, R. J. Schoelkopf, and L. Jiang, *Phys. Rev. Lett.* **125**, 110503 (2020).
- [78] U. L. Andersen, J. S. Neergaard-Nielsen, P. van Loock, and A. Furusawa, *Nat. Phys.* **11**, 713 (2015).
- [79] F. Reiter, A. S. Sørensen, P. Zoller, and C. A. Muschik, *Nat. Commun.* **8**, 1822 (2017).
- [80] I. Rojkov, D. Layden, P. Cappellaro, J. Home, and F. Reiter, *Phys. Rev. Lett.* **128**, 140503 (2022).